

# Memory in the Photon Statistics of Multilevel Quantum Systems

Felipe Caycedo-Soler and Ferney J. Rodriguez  
*Departamento de Física, Universidad de Los Andes,  
 A.A. 4976 Bogota, D.C., Colombia (South-America)*

Gert Zumofen  
*Laboratory of Physical Chemistry, ETH-Zurich, CH-8093 Zurich, Switzerland  
 (Dated: February 17, 2022)*

The statistics of photons emitted by single multilevel systems is investigated with emphasis on the nonrenewal characteristics of the photon-arrival times. We consider the correlation between consecutive interphoton times and present closed form expressions for the corresponding multiple moment analysis. Based on the moments a memory measure is proposed which provides an easy way of gaging the non-renewal statistics. Monte-Carlo simulations demonstrate that the experimental verification of non-renewal statistics is feasible.

PACS numbers: 03.65.Yz, 32.80.-t, 42.50.Ar, 42.50.Ct

The arrival times of photons emitted by single quantum systems have become a task of routine measurements [1–9]. Several methods are currently in use for the analysis of the recorded photon time traces, such as the second order field-correlation function [1–3, 10, 11], photon-number statistics [12, 13], exclusive and nonexclusive interphoton probability density functions (PDF) [3, 14–16], or Mandel’s Q-function [3, 4, 13, 17]. Usually, the PDF of photon-arrival times is considered to depend solely on the arrival time of the previous photon, assuming tacitly that photon emission is a renewal (semi-Markovian) process [14]. Consequently, multiple interphoton time PDFs are factorized and cast into products of one-interphoton time PDFs [3, 14]. In contrast, a nonrenewal process indicates a memory, since the photon-arrival time PDF depends not only on the arrival time of the previous but also on the arrival time of the photon before last, and consequently on the particular realization of the previous photons’ time trace [15, 16, 18].

For ensembles of microscopic photon sources the photon statistics is expected to be renewal, however, experiments reported on single and coupled quantum dots [6, 19–21], on single pairs of coupled molecules [8, 22, 23], and on two-state dynamics of single molecules [7] could be considered for the investigation of nonrenewal properties in the photon statistics. Recently, a renewal indicator was introduced for the study of conformational fluctuations of single molecules [24]. This indicator is closely related to Mandel’s Q-function and relies on the statistics of the number of photons recorded in a given time interval. In this paper we consider another technique which is based on the correlation between consecutive interphoton times. We apply a multiple-moment analysis of consecutive interphoton times and propose a measure  $\mathcal{M}$  for deviations from renewal statistics.

The time evolution of a multilevel quantum system interacting with the radiation vacuum can be given in

terms of the reduced density matrix  $\rho$  by ( $\hbar = 1$ ) [11, 15]

$$\dot{\rho} = \mathcal{L}\rho = i[\rho, H] + \sum_{i,j} \gamma_{ij} \left( S_i^- \rho S_j^+ - \frac{1}{2} [S_i^+ S_j^-, \rho]_+ \right), \quad (1)$$

where the Liouvillian  $\mathcal{L}$  consists of the Hamiltonian  $H$ , which includes the interaction with the classical driving field, and of dissipation in the Lindblad form. As usual,  $S_i^-$  ( $S_i^+$ ) are lowering (rising) operators for the  $i$ -th transition.  $\gamma_{ij}$  denote for  $i = j$  the spontaneous emission rates and for  $i \neq j$  cooperative decay rates deviating from zero if the difference of the two involved transition frequencies is smaller than the inverse radiation-bath correlation time,  $|\omega_i - \omega_j| \leq 1/\tau_c$  [18]. Assuming the rotating wave approximation,  $\mathcal{L}$  does not depend on time so that the evolution of  $\rho$  is given by  $\rho(t) = e^{\mathcal{L}t} \rho(0)$ , where  $\rho(0)$  denotes the state at time zero.

For the description of state collapses upon photon detection, several theoretical approaches, pioneered by the Monte-Carlo wave function technique [25], were developed. These approaches rely on quasi-continuous photon-emission measurements to introduce system states conditioned on whether a photon is detected or not [18, 26]. Accordingly, the Liouvillian is split into two terms [18]

$$\mathcal{L} = \mathcal{L}_c + \mathcal{R}, \quad (2)$$

where  $\mathcal{L}_c$  governs the time evolution of the conditioned and non-normalized density matrix  $\rho_c(t) = e^{\mathcal{L}_c t} \rho(0) = \mathcal{U}_c(t) \rho(0)$ , subject to a zero-photon outcome of the measurement up to time  $t$ . The second term in Eq. (2) represents the collapse (reset, recycling) operator  $\mathcal{R}$  [18] to reset the density matrix upon a photon detection event [16, 27]

$$\mathcal{R}\rho = \eta \sum_{i,j} \gamma_{ij} S_i^- \rho S_j^+. \quad (3)$$

The dimensionless detection efficiency  $\eta$  is introduced to account for the fact that a state collapse takes exclusively place when the emitted photon is also detected

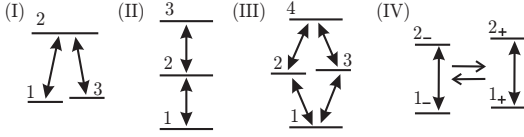


FIG. 1: Multi-level systems under consideration: (I) three-level  $\Lambda$ -system, (II) cascade three-level system, (III) four-level system motivated by a pair of interacting two-level systems, and (IV) a two level system jumping stochastically and radiationless between two states. Heavy arrows for laser-light driven and spontaneous radiation transitions and light arrows for radiationless transitions.

[16]. According to Eq. (2), also the conditioned Liouvillian  $\mathcal{L}_c = \mathcal{L} - \mathcal{R}$  depends on  $\eta$  in a unique way.  $\mathcal{R}$  operating on  $\rho_c(t)$  at random times generates a stochastic process and thus the average survival probability  $P_0(t)$  of no-photon detection up to time  $t$  is [11]

$$P_0(t) = \text{Tr} \{ \rho_c(t) \} = \text{Tr} \{ \mathcal{U}_c(t) \rho_0 \}, \quad (4)$$

provided that a photon was recorded at time zero. Correspondingly,  $\rho_0$  is the average state just after photon detection and is given by normalizing the collapsed stationary state,  $\rho_0 = \mathcal{R} \rho^{\text{ss}} / \text{Tr} \{ \mathcal{R} \rho^{\text{ss}} \}$ , where the stationary state satisfies  $\mathcal{L} \rho^{\text{ss}} = 0$ .

Recording the times of state collapses generated by repeated application of the operator  $\mathcal{R} \mathcal{U}_c(t)$  mimics the time traces of photon detection in a particular single quantum system experiment. The conditional density matrix right after the  $n$ -th photon detection of a sequence of exclusive detection times  $\{t_1, \dots, t_n\}$  with  $t_i \geq t_{i-1}$  is then given by

$$\rho_c(t_1, t_2, \dots, t_n) = \left[ \mathcal{T}_+ \prod_{i=1}^n \mathcal{R} \mathcal{U}_c(t_i - t_{i-1}) \right] \rho_0, \quad (5)$$

where the time ordering operator  $\mathcal{T}_+$  ensures that the operator at the latest time is on the far left. The trace of  $\rho_c(t_1, t_2, \dots, t_n)$  in Eq. (5) provides the detection PDF of a particular time sequence

$$p_n(\tau_1, \tau_2, \dots, \tau_n) = \text{Tr} \left\{ \left[ \mathcal{T}_+ \prod_{i=1}^n \mathcal{R} \mathcal{U}_c(\tau_i) \right] \rho_0 \right\}, \quad (6)$$

where  $\tau_i = t_i - t_{i-1}$  are interphoton times. Furthermore, the PDF  $P_2(t)$  of detecting a second photon at time  $t$ , given a detection event at any previous instance, follows from summing up all possible realizations of two consecutive interphoton times [15]

$$P_2(t) = \int_0^t p_2(t - \tau_1, \tau_1) d\tau_1. \quad (7)$$

Generally, referring to Eq. (6) the PDF  $P_n(t)$  of the  $n$ -th photon at time  $t$  results from the  $n - 1$  fold convolution of the operator  $\mathcal{R} \mathcal{U}_c(t)$ , where for completeness,  $P_1(t) = p_1(t)$ . For the quantitative analysis of  $p_n$ , we examine the moments to order  $m_i, i = 1, \dots, n$  for  $n$  consecutive detection intervals. These moments can readily

be calculated using a moment generating function technique in several dimensions

$$\begin{aligned} \mu_{m_1, \dots, m_n} &= \left( \prod_{i=1}^n \int_0^\infty d\tau_i \tau_i^{m_i} \right) p_n(\tau_1, \dots, \tau_n) \\ &= \text{Tr} \left\{ \left( \mathcal{T}_+ \prod_{i=1}^n (-1)^{(m_i+1)} m_i! \mathcal{R} \mathcal{L}_c^{-(m_i+1)} \right) \rho_0 \right\}, \end{aligned} \quad (8)$$

where, recalling, the ordering operator  $\mathcal{T}_+$  ensures that the operator at the latest time is on the far left. Eq. (8) allows for an easy numerical calculation of multiple moments. In case of renewal,  $\mathcal{R} \rho(t)$  does not depend on  $t$ , in other words the state after a collapse is independent of the state just before the collapse. Consequently,  $p_n(\tau_1, \dots, \tau_n)$  of Eq. (6) can be factorized in terms of the one-interphoton time PDF,  $p_n^{\text{R}}(\tau_1, \dots, \tau_n) = \prod_{i=1}^n p_1(\tau_i)$ , where the superscript R denotes renewal. Furthermore, the arrival PDF of the second photon is  $P_2^{\text{R}}(t) = p_1(t) * p_1(t)$ , where  $*$  indicates convolution and multiple moments reduce to products of individual moments

$$\mu_{m_1, \dots, m_n}^{\text{R}} = \prod_{i=1}^n \langle \tau_i^{m_i} \rangle = \prod_{i=1}^n \mu_{m_i}. \quad (9)$$

Differences between the PDFs  $p_n(\tau_1, \dots, \tau_n)$  and  $p_n^{\text{R}}(\tau_1, \dots, \tau_n)$ ,  $P_2(t)$  and  $P_2^{\text{R}}(t)$ , or between the moments of Eqs. (8) and (9) may be used to demonstrate whether the initial state  $\rho_0$  is recovered after photon emission and the process is renewal or whether the state-resetting depends on the current state and the process is nonrenewal. The deviation from renewal is a signature of the lack of information about the system state after photon emission and indicates the memory present in the correlation between consecutive photon-arrival times. Envisaging the experimental verification of NRS we concentrate on two consecutive time intervals and propose the following measure

$$\mathcal{M} = \mu_{1,1} / \mu_1^2 - 1, \quad (10)$$

which can be determined directly from the experimental time traces and can easily be predicted using Eq. (8).  $\mathcal{M}$  takes on both signs and an analysis of bi-valued waiting-time sequences indicate that tentatively  $\mathcal{M}$  is negative when shorter and longer waiting times are likely to occur alternately and is positive when both, shorter and longer waiting times are likely to be bunched.

The multiple moments of Eq. (8) and the measure  $\mathcal{M}$  of Eq. (10) represent the main result of this paper and we consider  $\mathcal{M}$  as a characteristic quantity complementary to other statistical measures, e.g. the photon coincidence probability (PCP)  $g^{(2)}(0)$ . We also studied the covariance of the functions  $P_2(t)$  and  $P_2^{\text{R}}(t)$ , however, such an analysis requires binning of the time traces and is therefore less direct for gaining information about the memory in the photon statistics.

To illustrate the NRS in photon counting we consider a representative set of level schemes, shown in Fig. 1.

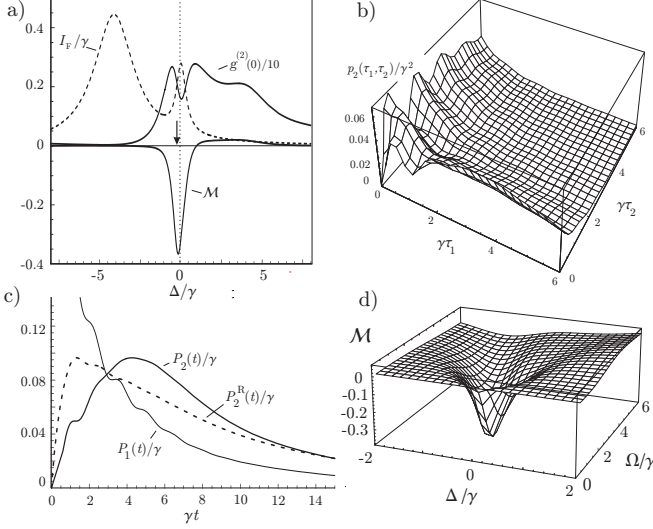


FIG. 2: The three-level cascade system. a) Memory  $\mathcal{M}$ , PCP  $g^{(2)}(0)$ , and fluorescence-excitation intensity  $I_F$  as a function of the laser detuning  $\Delta$ . The arrow indicates the  $\Delta$  value used in b) and c). b) Renewal and nonrenewal second-photon arrival PDF  $P_2^R(t)$  and  $P_2(t)$ , respectively, and one-photon arrival PDF  $P_1(t)$ . c) Two-photon arrival PDF  $p_2(\tau_1, \tau_2)$ . d) Memory  $\mathcal{M}$  as a function of the detuning  $\Delta$  and the Rabi frequency  $\Omega$ .

For the three-level  $\Lambda$ -system (I) renewal applies, because once a photon is detected the system is reset to the same mixed state, no matter the state before emission. In this respect, the  $\Lambda$ -system equals a two-level system which always collapses to the ground state. In contrast, NRS arises for systems (II-IV): For the three level cascade (II), upon the detection of a spectrally unresolved photon, the populations and coherences of the states  $|1\rangle$  and  $|2\rangle$  become proportional to the ones of  $|2\rangle$  and  $|3\rangle$  prior to emission, respectively [18]. In the four level cascade (III), the reset operator ladders populations and coherences down the levels:  $|4\rangle \rightarrow (|3\rangle, |2\rangle) \rightarrow |1\rangle$ . The non-cascade system (IV) shows a TLS flipping stochastically between two states. The flipping may be associated with changes of spectral and dynamical properties so that bunching of short and long interphoton times and thus NRS results. Summarizing, if the state after emission depends on the state prior to emission, the photon time traces obey NRS. The PCP can be discussed accordingly, namely, for system (I) it is zero, and is non-zero for systems (II) and (III). However, for system (IV) the PCP is zero although the process is nonrenewal in general.

We next discuss the level schemes (II-IV) in more detail. The Hamiltonian in Eq. (1) can be written as  $H = H_0 + \sum_i \frac{1}{2} \Omega_i (S_i^+ + S_i)$ , where  $\Omega_i$  is the Rabi frequency of the  $i$ -th transition resulting from the interaction with the classical driving field. For level scheme (II)

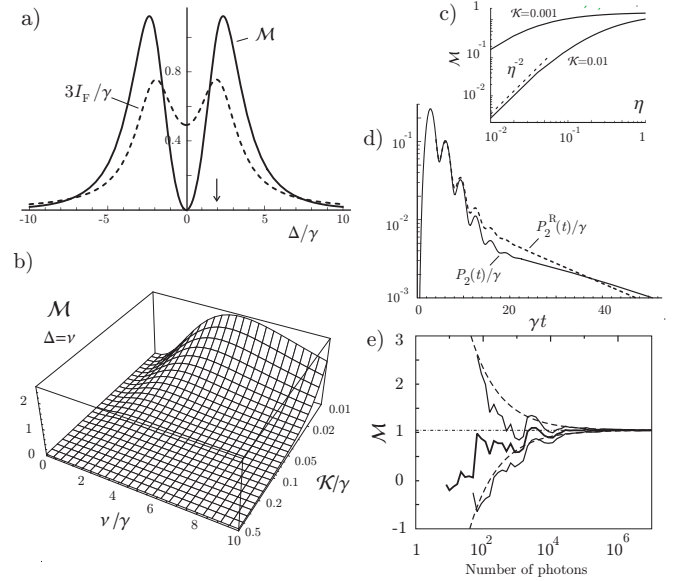


FIG. 3: Jumping two-level system. a)  $I_F$  scaled as indicated and  $\mathcal{M}$  as a function of the laser detuning, similarly as in Fig. 2a. The arrow indicates the detuning used in Fig. 2d. b)  $\mathcal{M}$  as function of  $\nu$  and  $\mathcal{K}$  on linear and log scales, respectively. c)  $\mathcal{M}$  as a function of the detection efficiency  $\eta$  on log-log scales for two values of  $\mathcal{K}$ . The dashed line for the  $\eta^{-2}$  dependence. d) Second-photon arrival time PDFs  $P_2^R(t)$  and  $P_2(t)$ . e)  $\mathcal{M}$  and confidence intervals  $\mathcal{M} \pm \sigma_{\mathcal{M}}$  as a function of the number of detected photons. Wiggly lines for Monte-Carlo simulations and dashed lines for predictions. The dash-dotted line gives the predicted value  $\mathcal{M} = 1.04$ .  $\Delta = \nu$  in panels b)-e).

we write for the zero-order Hamiltonian

$$H_0^{(II)} = -\delta_1 S_1^+ S_1^- - (\delta_1 + \delta_2) S_2^+ S_2^-, \quad (11)$$

where  $S_1^- = |1\rangle\langle 2|$  and  $S_2^- = |2\rangle\langle 3|$  are lowering operators with rising operators defined accordingly.  $\delta_1 = \omega_L - \omega_{21}$  and  $\delta_2 = \omega_L - \omega_{32}$  are differences between the laser frequency  $\omega_L$  and transition frequencies  $\omega_{ij}$ . Results are shown in Fig. 2 for the parameters:  $\Omega_1 = \Omega_2 = \Omega = 2\gamma$ ,  $\gamma_{11} = \gamma_{22} = \gamma$ ,  $\gamma_{12} = \gamma_{21} = 0$ ,  $\omega_{32} - \omega_{21} = 8\gamma$ , and  $\eta = 1$ . In Fig. 2a the excitation fluorescence intensity  $I_F = \text{Tr}\{\mathcal{R}\rho^{ss}\}$ , the PCP  $g^{(2)}(0) = \text{Tr}\{\mathcal{R}^2\rho^{ss}\}/I_F^2$ , and  $\mathcal{M}$  are compared as functions of the detuning  $\Delta = \frac{1}{2}(\delta_1 + \delta_2)$ . The fluorescence shows a maximum located approximately at resonance with the the lower transition ( $\delta_1 \simeq 0$ ), followed by a peak at  $\Delta \simeq 0$ , where coherent two-photon absorption and cascade emission are likely to occur. The intensity at resonance with the upper transition ( $\delta_2 \simeq 0$ ) is weak because of weak pumping of level 2. The PCP indicates photon antibunching in the range of the lower transition and photon bunching in the range of two-photon absorption and of the upper transition. In agreement with the above discussion,  $\mathcal{M}$  takes on negative values in the range of  $\Delta \simeq 0$ , where alternating short and long interphoton times are probable. At resonance with the upper transition,  $\mathcal{M}$  is weakly positive indi-

cating minor bunching of short and long waiting times.  $P_2(t)$  and  $P_2^R(t)$  displayed in Fig. 2b deviate considerably from each other and similarly a strong asymmetry is apparent in the PDF  $p_2(\tau_1, \tau_2)$  upon interchanging  $\tau_1$  and  $\tau_2$  demonstrated in Fig. 2c. In Fig. 2d  $\mathcal{M}$  is monitored as a function of  $\Delta$  and  $\Omega$ . A minimum close to  $\Delta \simeq 0$  and  $\Omega \simeq 2\gamma$  is clearly visible. We have found that  $|\mathcal{M}|$  drops roughly as  $\eta^{-2}$  so that the experimental verification of NRS requires a high detection efficiency.

Motivated by recent investigations of pairs of identical and interacting quantum systems [8, 21, 23] we studied system (III). Depending on the parameters the results (not shown here) were similar to those of system (II) which is obvious when states 2 and 3 are superposition Dicke states [26, 28], so that the behavior is governed by the  $1 \leftrightarrow 2$  and  $2 \leftrightarrow 4$  transitions or  $1 \leftrightarrow 3$  and  $3 \leftrightarrow 4$  transitions.

We finally report on the non-cascade, jumping two-level system (IV) where the  $\pm$  states indicate for instance two different molecular, or lattice nuclear configurations [7, 17], spectral diffusion of ultracold molecules in condensed media [29], or two different spin configurations. The dynamics is described by extending the density operator,  $\rho = (\rho_-, \rho_+)^T$ , and correspondingly the Liouvillian and reset operators [17]

$$\mathcal{L}^{(IV)} = \begin{pmatrix} \mathcal{L}_- - \mathcal{K}_- & \mathcal{K}_+ \\ \mathcal{K}_- & \mathcal{L}_+ - \mathcal{K}_+ \end{pmatrix}, \mathcal{R} = \begin{pmatrix} \mathcal{R}_- & 0 \\ 0 & \mathcal{R}_+ \end{pmatrix}, \quad (12)$$

where  $\mathcal{K}_\pm$  denote the jumping rates between the two states and where  $\mathcal{L}_\pm$  and  $\mathcal{R}_\pm$  are the Liouvillian and resetting operators of the two states. For illustration we assume the full symmetric case where only the transition frequencies are different for the two states. Thus the system is described by the Hamiltonian  $H_\pm = (-\Delta \pm \nu)S_\pm^\dagger S_\pm + \frac{1}{2}\Omega(S_\pm + S_\pm^\dagger)$ , where  $\Delta$  and  $\nu$  are laser detuning and frequency displacements from the transition center, respectively. Furthermore,  $\gamma_\pm = \gamma$ ,  $\mathcal{R}_\pm = \mathcal{R}$ , and  $\mathcal{K}_\pm = \mathcal{K}$ . Numerical results are shown in Fig. 3 for the parameters  $\Omega = 2\gamma, \nu = 2\gamma, \eta = 1, \mathcal{K} = \gamma/100$ , except when they appear as variables or are specially indicated.  $\mathcal{M}$  is positive throughout all calculations and peaks close to the resonances of the two states. Fig. 3b indicates large positive  $\mathcal{M}$  for  $\mathcal{K} \ll \gamma$  and for  $|\Delta| \simeq |\nu|$ . Fig. 3c shows how the  $\eta$  dependence of  $\mathcal{M}$  crosses over to the asymptotic  $\eta^{-2}$  behavior and how the crossover is shifted to lower values of  $\eta$  with decreasing  $\mathcal{K}$ . The second-photon arrival PDFs  $P_2^R(t)$  and  $P_2(t)$  in Fig. 3d differ only at longer times which indicates that these quantities are not appropriate for providing evidence of NRS.

To demonstrate the experimental feasibility of measuring  $\mathcal{M}$ , we report Monte-Carlo simulation results [11, 25]. Choosing a random number  $r$  distributed uniformly in  $[0, 1]$ , the detection time  $t_n$  of the  $n$ -th photon follows

from the condition

$$\text{Tr} \{ \mathcal{U}_c(t_n - t_{n-1}) \hat{\rho}_c(t_1, \dots, t_{n-1}) \} = r, \quad (13)$$

where  $\hat{\rho}_c$  is the normalized conditioned density matrix of Eq. (5). By resetting and normalizing the state at  $t_n$ , the initial state of the next interphoton cycle is obtained. Fig. 3e shows, how  $\mathcal{M}$  converges as a function of the photon number to the predicted value. Also presented are confidence intervals  $\mathcal{M} \pm \sigma_{\mathcal{M}}$ , which are estimated from the variance, assuming statistical independence of the moments:  $\sigma_{\mathcal{M}}^2 = \sigma_{\mu_{1,1}}^2 / \mu_1^4 + 4(\mu_{1,1} / \mu_1^3)^2 \sigma_{\mu_1}^2$ , where  $\sigma_{\mu_1}^2 = \mu_2 - \mu_1^2$  and  $\sigma_{\mu_{1,1}}^2 = \mu_{2,2} - \mu_{1,1}^2$ .

The experimental investigation of the NRS requires the measurement of two consecutive intervals, so that the arrival times of three consecutive photons have to be recorded. Depending on the time scale, this can be achieved using a single detector, however, for time scales shorter than the detectors' dead time, at least three detectors are needed. A comprehensive description of experimental data has to account for the detectors' dead time and for the ubiquitous background photons.

In conclusion, we have shown that NRS is plausible in the fluorescence of multi-level systems and that the indicator  $\mathcal{M}$ , proposed for the identification of the non-renewal property, is experimentally feasible. For cascade systems  $\mathcal{M}$  may be small at low detection efficiency, so that advanced experimental techniques are required, while for non-cascade multi-level systems  $\mathcal{M}$  may be large also at low detection efficiency.

We thank V. Sandoghdar for stimulating discussions. F.C.S. thanks the ETH-Zurich for the hospitality and the financial support from COLCIENCIAS No. 1204-05-11408 and Banco de la República.

- 
- [1] H.J. Kimble, M. Dagenais, L. Mandel, Phys. Rev. Lett. **39**, 691 (1977).
  - [2] Th. Basché et al., Phys. Rev. Lett. **69** 1516 (1992).
  - [3] L. Fleury et al., Phys. Rev. Lett. **84**, 1148 (2000).
  - [4] F. Diedrich and H. Walther, Phys. Rev. Lett. **58** 203 (1987).
  - [5] J. Enderlein, D. I. Robbins, W. P. Ambrose, and R. A. Keller, J. Phys. Chem. A **102**, 6089 (1998).
  - [6] B.D. Gerardot et al., Phys. Rev. Lett. **95**, 137403 (2005).
  - [7] A. Zumbusch et al., Phys. Rev. Lett. **70**, 3584 (1993).
  - [8] C. Hettich et al., Science **298**, 385 (2002).
  - [9] G. Zumofen, J. Hohlbein, C.G. Hübner, Phys. Rev. Lett. **93**, 260601 (2004).
  - [10] I.S. Osad'ko, J. Luminisc. **87**, 184 (2000).
  - [11] M.B. Plenio and P.L. Knight, Rev. Mod. Phys. **70**, 101 (1998).
  - [12] I.S. Osad'ko, JETP Lett. **85**, 550 (2007).
  - [13] L. Mandel, Opt. Lett. **4**, 205 (1979).
  - [14] G.S. Agarwal, Phys. Rev. A **15**, 814 (1977).
  - [15] P. Zoller, M. Marte, and D.F. Walls, Phys. Rev. A **35**, 198 (1987).

- [16] H.J. Charnichael et al., Phys. Rev. A **39** 1200 (1989).
- [17] Y. He and E. Barkai, Phys. Rev. Lett. **93** 68302 (2004).
- [18] G.C. Hegerfeldt, Phys. Rev. A **47**, 449 (1993).
- [19] T. Unold, et al., Phys. Rev. Lett. **94**, 137404 (2005).
- [20] J. Persson et al., Phys. Rev. B **69**, 233314 (2004).
- [21] M. Bayer, et al, Science **291**, 451 (2001).
- [22] A.J. Berglund, A. C. Doherty, and H. Mabuchi, Phys. Rev. Lett. **89**, 068101 (2002).
- [23] C.G. Hübner et al., Phys. Rev. Lett. **91**, 093903 (2003).
- [24] J. Cao, J. Phys. Chem. B **110**, 19040 (2006).
- [25] J. Dalibard et al., Phys. Rev. Lett. **68**, 580 (1992).
- [26] A. Beige and G.C. Hegerfeldt, Phys. Rev. A **58**, 4133 (1998).
- [27] F. Sanda and S. Mukamel, Phys. Rev. A **71**, 33807 (2005).
- [28] U. Akram, Z. Ficek, and S. Swain, Phys. Rev. A **62**, 13413 (2000).
- [29] I.S. Osad'ko and E. V. Kohts, Optics and Spectroscopy **94**, 949 (2003).